

Modeling startup and shutdown transient of the microlinear piezo drive via ANSYS

A V Azin¹, E P Bogdanov², S V Rikkonen¹, S V Ponomarev¹ and
A M Khramtsov¹

¹ Tomsk State University, 36, Lenina Ave., Tomsk, 634050, Russia

² Tomsk Polytechnic University, 30, Lenina Ave., Tomsk, 634050, Russia

E-mail: epbogdanov@mail.ru

Abstract. The article describes the construction-design of the micro linear piezo drive intended for a peripheral cord tensioner in the reflecting surface shape regulator system for large-sized transformable spacecraft antenna reflectors. The research target –the development method of modeling startup and shutdown transient of the micro linear piezo drive. This method is based on application software package ANSYS. The method embraces a detailed description of the calculation stages to determine the operating characteristics of the designed piezo drive. Based on the numerical solutions, the time characteristics of the designed piezo drive are determined.

1. Introduction

The problem of reducing the spacecraft (SC) system mass-dimension parameters is especially acute in the space field. One current solution consists in replacing electro-mechanical drives in different SC units with piezo drives which, in its turn, would decrease the mass-dimension parameters n-fold times [1, 2].

The peripheral cord tensioner unit (PCTU) in the reflecting surface shape regulator system for large-sized transformable spacecraft antenna reflectors provides the preliminary tension of the spacecraft reflector surface itself. The peripheral cord tension is $F_{\text{tens}} = 300$ N, the unit mass – 250 g, the total reflector spoke mass – 35 kg, cord displacement $X_{\text{tens}} = 0.5$ m. Cord displacement at 0.5m could be only in case of the animated regime of operating micro linear piezo drives (MLPD) [3, 4].

Studying the types of MLPD transient involves:

- establishing the animated regime of operating MLPD within PCTU to determine the operation transient behavior during MLPD startup and shutdown;
- preventing startup transient as a consequence of the impulse regime with temporary vibration displacement which is significantly exceeds the certified MLPD values and could result in the emergency mode of the system itself.

Modeling of startup and shutdown transient of the micro linear piezodrive method is described step-by-step via application software package ANSYS.

2. Problem statement

Generally, the MLPD system status is described by elastodynamics equations. Let us consider domain Ω with boundary S . Let us find displacement field $\vec{u}(x_1, x_2, x_3, t)$ as a function of spatial coordinates



$x = (x_1, x_2, x_3)$, changing in domain Ω of 3D Euclidean space and time t [5-9]. Differential continuum equations are obtained from static equilibrium equations, including mass inertia forces:

$$\frac{\partial \sigma_{ij}}{\partial x_j} + \rho F_i = \rho \frac{\partial^2 u_i}{\partial t^2}. \quad (1)$$

The deformation and displacement connection is

$$\varepsilon_{ij} = \frac{1}{2} \left(\frac{\partial u_i}{\partial x_j} + \frac{\partial u_j}{\partial x_i} \right). \quad (2)$$

To simulate the mechanical behavior in tension, Hooke's law is used:

$$\begin{aligned} \sigma_{ij} &= \lambda \theta \delta_{ij} + 2\mu \cdot \varepsilon_{ij}, \\ \theta &= \varepsilon_{11} + \varepsilon_{22} + \varepsilon_{33} = \bar{\varepsilon}, \end{aligned} \quad (3)$$

where, δ_{ij} – Kronecker symbol; u_i , σ_{ij} , ε_{ij} – components of the displacement vector, second stress tensor of Piola-Kirchhoff; deformation stress tensor; μ , λ – Lamé parameters; ρ – material density; F_i – mass force.

Boundary conditions: if the body surface includes two parts:

$$\begin{aligned} S &= S_1 + S_2, \\ u_i(\bar{x}) &= 0, \bar{x} \in S_1, \end{aligned} \quad (4)$$

$$n_k \sigma_{kj} \left(\delta_{ij} + \frac{\partial u_i}{\partial x_j} \right) = 0, \bar{x} \in S_2. \quad (5)$$

Initial conditions: at $t = 0$, the displacement field and velocity are assumed to be

$$\begin{aligned} u(x, 0) &= u_0(x), \\ \frac{\partial u}{\partial t}(x, 0) &= \bar{v}_0(x). \end{aligned} \quad (6)$$

For piezo-electrical bodies, equation (1) is written as straight-line and reverse piezoeffect equation (7, 8) and constrained electrostatics equation (9):

$$\sigma_{ij} = C_{ijkl}^E \varepsilon_{kl} + \xi C_{ijkl}^E \varepsilon_{kl} - e_{ij} U_i, \quad (7)$$

$$D_i = e_{ijk} \varepsilon_{jk} + \varepsilon_{ij}^S U_j, \quad (8)$$

$$U = -\text{grad} \phi, D = 0, \quad (9)$$

where, D – the electrostatic field induction vector; U – the electrostatic field intensity vector; ϕ – electrostatic potential; C^E – the elastic piezo ceramic material modulus; e – the piezoelectrical modulus; ε^S – dielectric constants; ξ – the introduced coefficient to describe damping in the Rayleigh solid medium (viscoelastic losses).

Temperature components are excluded from the equation systems as operating conditions of the micro linear drive are considered to be isothermal.

3. The mathematical calculation model for MLPD

The basic steps in engineering analysis through the finite element method (FEM) are the following:

1. creating a geometrical model (CAD): an actual physical model of the investigated object is developed and parametrized;
2. creating an idealized model, i.e. moving from an actual physical model to a changed (simplified) mathematical model;
3. creating a discrete model (FEM), corresponding to constrained degree-of-freedom, i.e. idealized model discretization: physical material properties are given and splitting model grid parameters are set;
4. solving equation systems, corresponding to the selected analysis type (modal analysis, harmonic analysis, transient analysis);

5. analyzing obtained results.

Let us consider the following case study by applying the above-mentioned algorithm.

3.1 CAD model development

MLPD includes a framework, an adjustment screw, PZT Stack, a cheek with an oscillator element, a pushrod and a resilient spacer (Figure 1a). The CAD model of the MLPD construction-design is illustrated in figure 1b. The framework impact on other MLPD elements was simulated by constraint conditions: attaching the lower PZT Stack boundary and the upper resilient spacer boundary. The load on MLPD is simulated by the point mass attached to the upper pushrod surface. As the described problem is axisymmetric, only $\frac{1}{4}$ of the MLPD construction is considered.

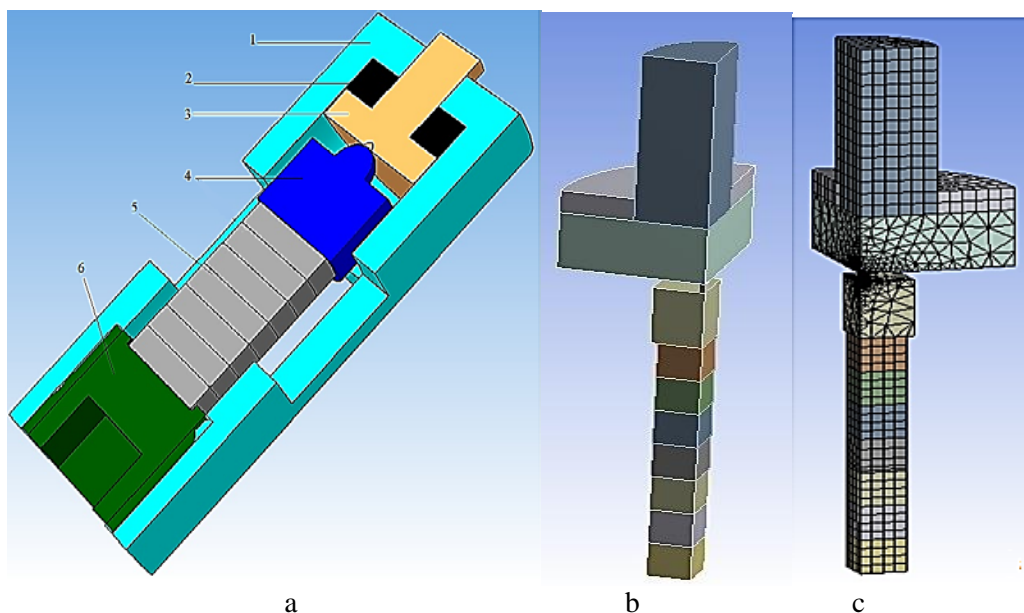


Figure 1. MLPD Modeling: a – overview; b – CAD model; c – FE model. 1– framework, 2 – resilient spacer, 3 – pushrod, 4 – cheek with oscillator element, 5 – PZT Stack, 6 – adjustment screw.

3.2 The finite element model

The finite element model (FEM) is designed on the basis of the geometrical model. To visualize the stress-strain state (SSS) of construction elements when subjected to loads, it is necessary to reduce the size of the elements in positions of likely maximum stress. In MLPD, it is the cheek-oscillator and the oscillator-pushrod contact zone. Such tools as line partitioning and boundary splitting offer this possibility. The finite element model of MLPD is illustrated in figure 1c showing the reduction of elements in the zone of likely maximum stress. The number of elements in presented FEM of MLPD is 5582.

The authors have developed a mathematical calculation model of the MLPD mechanical system in order to determine what materials are suitable for the mechanical cheek-oscillator-pushrod contact. Based on this model, the MLPD reinforcement element materials were determined to improve MLPD operation reliability and quality. In this case, the following materials were considered for the described MLPD construction model: cheek-steel, oscillator-steel, pushrod-plexiglas, spacer-rubber and PZT Stack-piezoelectric ceramics.

The material properties in calculation, presented in table 1, are reference data. The PZT Stack APM-2-7 was used in the MLPD construction. This PZT Stack embraces 7 PZT blocks. These PZT blocks are oriented towards the direction opposite to each other.

Table 1. Material properties in calculation

Material	Density, kg/m ³	Modulus of elasticity, Pa	Poisson ratio
Steel	7800	$2.1 \cdot 10^{11}$	0.29
Plexiglas	1190	$3 \cdot 10^9$	0.33
Rubber	1200	$5 \cdot 10^6$	0.5

Calculation data of piezo-ceramics (used in APM-2-7) have been received from the producer. Piezo-ceramics properties are depicted in table 2.

Table 2. Piezo-ceramics properties

Material properties	Value
Density, kg/m ³	7600
Planar Q-factor	70
Dielectric constant, F/m	$\varepsilon_{xx}^S = 2100; \varepsilon_{zz}^S = 1300$
Modulus of elasticity (anisotropic material), N/m ²	$C_{11}^E = 1.1 \cdot 10^{11}; C_{21}^E = 6.1 \cdot 10^{10}; C_{22}^E = 1.1 \cdot 10^{11};$ $C_{31}^E = 5.8 \cdot 10^{10}; C_{33}^E = 1.01 \cdot 10^{11}; C_{11}^E = 1.1 \cdot 10^{11};$ $C_{44}^E = 1.8 \cdot 10^{10}; C_{55}^E = 1.1 \cdot 10^{11}; C_{11}^E = 2.45 \cdot 10^{10}$
Piezoelectric modulus	$d_{31} = -190 \cdot 10^{-12}; d_{33} = 450 \cdot 10^{-12}; d_{15} = 400 \cdot 10^{-12}$

The next stage in calculation model plotting is the application of loads and introducing constraint conditions.

In actual conditions, the pushrod presses the spacer which is attached to (glued on) the MLPD frame work surface. Accordingly, fastening the nodes on the spacer surface in all three axes simulates this situation. The lower PZT Stack boundary is also rigidly fixed so as the force arising from input voltage by law $U(t) = U_0 \cdot \sin(f \cdot t)$ (where, U_0 – the amplitude applied to PZT Stack, equals 100 V; f – frequency; t – time), is transferred to the remaining MLPD elements.

The following factors are also considered: the load of displacement of reflector spokes and the spoke mass of 35 kg. This load is the point mass attached to the upper pushrod edge.

Equal values $\beta = 4 \cdot 10^{-5}$ were introduced into the damping MLPD system value. This value was determined according to the method described in ANSYS documents [10], applying the dominant oscillation frequency which, in its turn, involves the maximum ratio of effective mass to total mass.

3.3 Calculation results

The MLPD construction-design was considered. The following materials were used for the system elements: steel, piezoelectric ceramics, plexiglas and rubber. MLPD was examined under normal operation conditions, i.e. electrical connection and a sine wave signal of 100 V amplitude.

The modal analysis was conducted to determine the resonant frequencies at which MLPD executes the maximum displacement along a Z-direction. The following modes were obtained: 1 – 145 Hz and 6 – 13520 Hz.

The next calculation stage involved harmonic analysis. Based on the calculation results the following factor was determined: frequency at which the displacement of the pushrod is maximum: $f_0 = 140$ Hz, $X = 28.1 \cdot 10^{-6}$ m. The calculation results are depicted in figure 2 – the dependence of the pushrod displacement amplitude value on the set signal frequency from PZT Stack.

The last mathematical calculation stage involves the transient analysis. The analysis results are displacement diagrams reflecting the information on the node displacements on the upper pushrod edge where voltage is applied to MLPD PZT Stack (Figure 3) and where voltage is applied to MLPD PZT Stack lining (Figure 4). To visualize MLPD start-up and shut-off transient more exactly, the voltage value applied to the PZT Stack is changed in three-time intervals:

1. First time interval ($t = [0; 0.01]$ s) – stress on lining equals 0.

2. Second time interval ($t = [0.01; 0.37]$ s) – the voltage being applied to PZT Stack lining $U = U_0 \cdot \sin(2 \cdot \pi \cdot f_0 \cdot t)$, where U_0 – the amplitude of applied voltage ($U_0 = 100$ V), f_0 – resonant frequency ($f_0 = 140$ Hz). The MLPD start-up moment is simulated.
3. Third time interval ($t = [0.37; 1.5]$ s) – stress on lining equals 0. The MLPD shut-off moment is simulated.

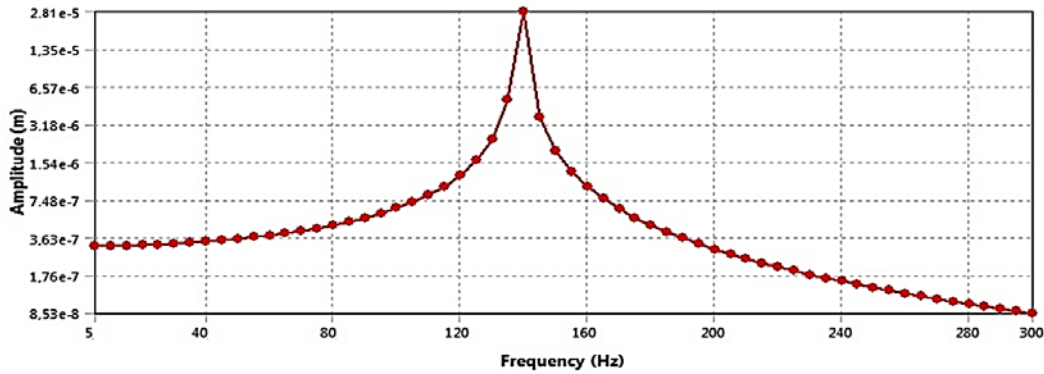


Figure 2. Dependence of the pushrod displacement amplitude value on the set signal frequency from PZT Stack.

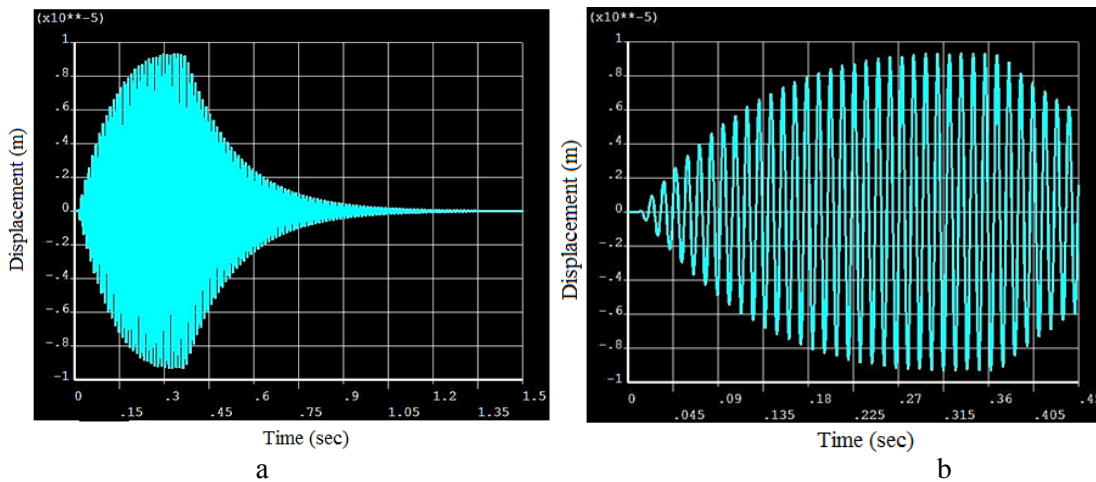


Figure 3. Start-up and shut-off transient of MLPD. Displacement along the upper MLPD pushrod boundary: a – complete process; b – process start-up.

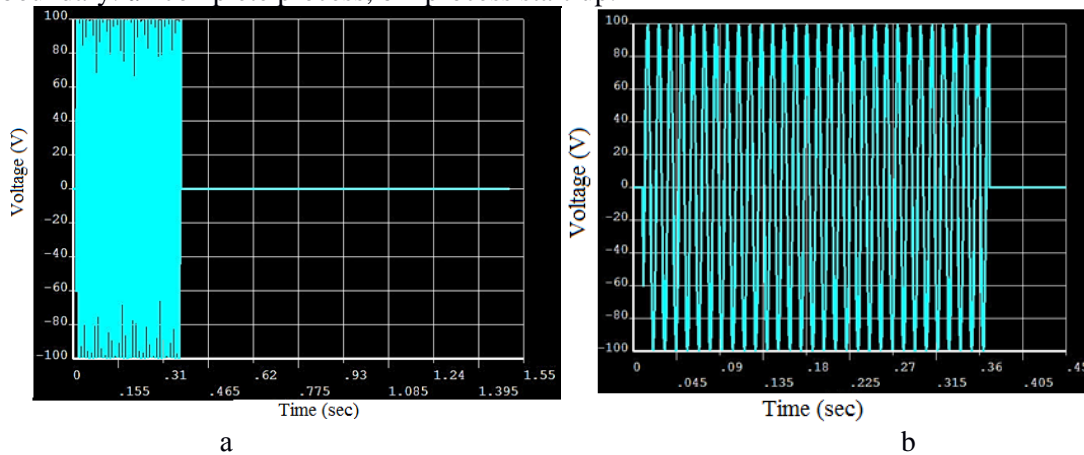


Figure 4. Start-up and shut-off transient of MLPD. The voltage in MLPD PZT Stack lining: a – complete process; b – process start-up.

The calculation results of MLPD start-up showed that the above-mentioned MLPD at a load of 35 kg requires 0.23 s to operate in a steady-state mode (Figure 4). The calculation results of MLPD shut-off showed that 0.98 s is required in damping the oscillations (Figure 4).

4. Conclusion

The modeling procedure of the startup and shutoff micro linear piezo drive has been developed.

This procedure includes a detailed description of the calculation stages to determine the operating characteristics of the designed piezodrive.

Based on numerical equations, the time characteristics for the designed micro linear piezodrive were determined. This, in its turn, made it possible to select the optimal operating regime for the micro linear piezodrive under the animated operating regime.

Acknowledgments

This work was financially supported by the Ministry of Education and Science of Russia; unique identifier RFMEFI57814X0060.

References

- [1] Park S 2011 *Single vibration mode standing wave tubular piezoelectric ultrasonic motor* (Toronto: Ryerson University)
- [2] Wang Z, Li T and Cao Y 2013 *Aerospace Science and Technology* **26** 160
- [3] Ponomarev S V, Rikkonen S V and Azin A V 2014 *News of Higher Educational Institutions. Physics* **2** 196
- [4] Ponomarev S V, Rikkonen S V and Azin A V 2015 *Tomsk State Univ. J. of Mathem. and Mechanics* **2(34)** 86
- [5] Abramenko T, Gorish A, Bogush M and Mitko V 2003 *Proc. of the Tenth Int. Congress on Sound and Vibration* (Stockholm) vol 3 (Stockholm: International Institute of Acoustics and Vibration) p 951
- [6] Bogush M 2014 *Design of piezoelectric sensors based on spatial electrical and thermoelastic models* (Moscow: Technosphaera publishing house)
- [7] Davoudi S 2012 *Effect of Temperature and Thermal Cycles on PZT Ceramic Performance in Fuel Injector Applications* (Toronto: Department of Mechanical and Industrial Engineering University)
- [8] Bogush M and Pikalev E 2008 *Izvestiya SFedU. Engineering sciences* **2(79)** 74
- [9] Bogush M 2008 *Izvestiya SFedU. Engineering sciences* **6** 18
- [10] 2013 Matrix resistance *Ansys Help Viewer* 15.0